

An Nb-doped Nickel Oxide–Carbon Nanotubes Composite-Enhanced Electrochemical DNA Biosensor for Detection of Lead(II) Ion

Daiwu Chen¹, Fenfang Deng², Cong Ding², Yu Wang^{3,*}, He Li^{2,*}

¹Department of Pharmacology, Shaoyang Medical College, Shaoyang 422000, China

²School of Chemistry and Environment, South China Normal University, Guangzhou 510006 China

³Department of Pathology, Zhujiang Hospital, Southern Medical University, Guangzhou 510282, China

*E-mail: analchemlh@163.com, doctorwylh@163.com

Received: 15 August 2015 / *Accepted:* 19 September 2015 / *Published:* 30 September 2015

A novel niobium doped nickel oxide nanoparticle (NbNiO) was synthesized by sol-gel method and was applied to fabricate DNA biosensor for detection of Pb²⁺ in water sample for the first time. The amino-modified G-rich DNA probes were immobilized on the surface of CH-NbNiO-MWCNTs/ITO electrode by the covalent interaction between the amino of DNA and the carboxyl of MWCNTs. When the lead (II) ion (Pb²⁺) interacted with the G-rich DNA, it will induce the DNA conformational to switch from a random-coil to a G-quadruplex resulting in an increase of alternating current impedance. On the basis of this, we developed an impedance biosensor for the detection of Pb²⁺. The results showed that the synergistic effect of the synthesized NbNiO nanoparticles and MWCNTs could improve the performance of this DNA biosensor. Under optimal conditions, the fabricated DNA biosensor possess a wide linear range of 1.0×10⁻¹⁰ to 1.0×10⁻⁵ M (correlation coefficient, R=0.998) and a low detection limit of 7.51 ×10⁻¹² M (3σ).

Keywords: Niobium doped nickel oxide, Electrochemical DNA biosensor, Lead (II) ion

1. INTRODUCTION

Lead is one of the most toxic metallic pollutants and can cause renal malfunction and inhibit brain development. Once it was absorbed by human body, it would cause significant physiological and neurological effects on humans, even at low levels, particularly for vulnerable populations such as children [1-2]. Therefore, an accurate and sensitive method for the detection of lead (II) ion (Pb²⁺) is of

great significance. The conventional methods including atomic absorption spectrometry [3-5], inductively coupled plasma mass spectrometry[6-8], anodic stripping voltammetry [9-11] and atomic fluorescence spectrometry[12-13] have been employed for the detection of Pb^{2+} . However, some of them were time-consuming, tedious sample pretreatment process and needed expensive apparatus. Recently, considerable efforts have been undertaken to develop novel electrochemical methods for the detection of Pb^{2+} based on oligonucleotides, DNA enzyme, polymers, small molecules and functional nanoparticles[14-16]. The electrochemical method possesses high sensitivity, simplicity, low cost and easily to miniaturization. Therefore the development of electrochemical biosensors for detection of Pb^{2+} ions has great potential applications in field monitoring.

With in-depth study of the interaction between DNA molecules and metal ions, functionalized DNA molecules gradually become effective tool for Pb^{2+} detection. Three types of DNA molecules (8-17 DNAzyme, GR-5 DNAzyme and G-rich DNA) affinity to Pb^{2+} have been reported [15-17]. However, DNAzyme is vulnerable to in vivo detection or complex systems when it comes to practical use [18]. So, it is necessary to develop the G-rich DNA electrochemical sensors for the detection of Pb^{2+} .

Carbon nanotube has been widely applied in the field of electrochemical biosensors because of its good biocompatibility, high mechanical strength, excellent magnetic property and wide electrochemical window[19]. And chitosan (CH) is used widely as an immobilization matrix in electrochemical biosensors due to its excellent film-forming ability, biocompatibility, mechanical strength, nontoxicity and hydrophilicity [20].

Metal oxide nanoparticles, such as ZnO [21], SnO₂ [22], In₂O₃ [23], NiO[24], CdO [25] and so on, have drawn chemist's attention in recent years due to their unique physical and chemical properties. Among them, the NiO has received intensive attention because of its good thermal sensitivity, electrically induced optical, catalytic activity and electrochemical activity [26], and widely applied in battery electrodes, transparent electronics, color changing electronics components and the function of the chemical sensors, electrochemical capacitor sensor layer and high-performance catalyst[27]. When NiO is doped with other metal elements, its electrical properties can be improved because the electrical transport is primarily associated with Ni²⁺ vacancies. Each Ni²⁺ vacancy in the lattice causes the transformation of two Ni²⁺ into two Ni³⁺ for meeting charge neutrality, and this transformation induces a local lattice distortion[28,29].

In this paper, the nanocomposite of NbNiO nanoparticles, carboxylic group- functionalized multi-walled carbon nanotubes and chitosan was immobilized on the indium tin oxide electrode and formed a nanocomposite film with a large specific surface area. Then amino-modified G-rich DNA probes were immobilized on the surface of CH-NbNiO-MWCNTs/ITO electrode by the interaction between the amino of DNA and the carboxyl of MWCNTs. Pb^{2+} could induce the conformation of G-rich DNA to switch from a random-coil to G-quadruplex, and result in an increase of alternating current impedance. On the basis of above mentioned, we developed an impedance biosensor for the detection of Pb^{2+} in real water samples.

2. EXPERIMENTAL

2.1 Reagents and materials

Niobium acid ammonium oxalate hydrates was obtained from Sigma-Aldrich (USA). MWCNTs was purchased from Shenzhen Nanotech Port Co., Ltd. Nickel nitrate, ammonium metavanadate, tetrabutyl titanate, manganese nitrate, citric acid, chitosan, sodium dihydrogen phosphate, disodium hydrogen phosphate, N-hydroxysuccinimide (NHS), B-yl(3-dimethyl-propyl) carbodiimide hydrochloride (EDC), Chitosan (CH) and other chemicals were purchased from Aladdin Reagent Company (Shanghai, China). The sequence 5'-NH₂-GGAAGGTGTGGAAGG-3' purified via polyacrylamide gel electrophoresis (PAGE) was synthesized by Invitrogen (Shanghai, China).

2.2 Apparatus

Scanning electron micrograph (SEM) was obtained on Zeiss Ultra55 field emission scanning electron microscope (Carl Zeiss, Germany). X-ray diffraction (XRD) was performed with Bruker D8 advance (Bruker, Germany). Thermogravimetry (TG) was carried out on simultaneous thermal analyzer (STAA449/3/MFC/G, NETZSCH). High-temperature tube furnace was used for Electrochemical measurements were recorded using an Autolab Potentiostat/Galvanostat (Metrohm). A conventional three-electrode cell with an Ag/AgCl reference, a platinum wire counter and the modified ITO as the working electrodes were used.

2.3 Synthesis of NbNiO nanoparticles

The NbNiO nanoparticles were synthesized by sol-gel method [30]. A certain amount of nickel nitrate and niobium acid ammonium oxalate hydrates were dissolved into deionized water, respectively, and simultaneously added dropwise into citric acid solution. Then specific content of nitric acid and aqueous ammonia were added to adjust the pH of the above solution to 1. Subsequently, the resulted solution was heated and stirred at 70°C to slowly evaporate the deionized water until a highly viscous transparent green sol was achieved. After that, the sol was transformed into oven, and heated at 110 °C for 24 h. A swell green NbNiO precursor was obtained. Eventually, the as-synthesized precursors were ground and then calcined in air at 400°C for 4 h to obtain the nanoparticles of NbNiO. The samples vanadium doped NiO (VNiO), titanium doped NiO (TiNiO) and manganese doped NiO (MnNiO) were prepared at similar procedures.

2.4 The preparation of MWCNTs

The MWCNTs were prepared according to the literature method [31] with appropriate modification. 0.2 g multi-walled carbon nanotubes were added to 50 mL of mixed acid HNO₃-H₂SO₄ (v/v, 3:1) with ultrasonic treatment for 0.5 h to make the MWCNTs disperse in the acid completely. Subsequently, the mixture was purified through refluxing for 6 h at 80°C. Then the resulting product

was separated by membrane filtration and washed with distilled water to neutral. Finally, the obtained carboxylic group-functionalized multi-walled carbon nanotubes (MWCNTs) was dried under vacuum at 60°C for 24 h.

2.5 Fabrication of electrochemical DNA biosensor

The fabrication procedure of electrochemical DNA biosensor referred to our previous literature[32]. The DNA biosensor was prepared as follows: (i) prior to modification, the ITO substrates were soaked in an ultrasonic bath successively with acetone, absolute alcohol and distilled water for 5 min each time, and then dried at room temperature; (ii) 50 mg of CH was dissolved into 10mL of 1% (vol.%) acetic acid solution to form a transparent CH solution; then 6 mg of as-synthesized NbNiO nanoparticles and 4 mg MWCNT-COOH were dispersed into above solution and sonicated for 6h to obtain a uniform gel of CH-NbNiO-MWCNTs; (iii) 10 μ L of above nanocomposite was pipetted onto the surface of the cleaned ITO electrode and dried at room temperature to get a modified electrode denoted as CH-NbNiO-MWCNTs/ITO; (iv) The CH-NbNiO-MWCNTs/ITO electrode was placed in a mixture of NHS and EDS at 40 °C for 1 h, followed by washing with deionized water and drying at room temperature; (v) Immobilization of NH₂-ssDNA probes was performed by pipetting 10 μ L of 1.0 μ M NH₂-ssDNA on the CH-NbNiO-MWCNTs/ITO surface for dryness at room temperature, followed by washing with PBS solution (pH 7.0) and ultrapure water to remove the un-immobilized NH₂-ssDNA, the obtained electrode was denoted as ssDNA/CH-NbNiO-MWCNTs/ITO.

2.6 The formation of G-quadruplex induced by Pb²⁺

The ssDNA/CH-NbNiO-MWCNTs/ITO electrode was immersed into different concentrations of Pb²⁺ solution (0.1 M PBS, pH 7.0) for 5 min at 90°C, followed by cooling to room temperature within 1 h and keeping at room temperature for 1 h to ensure G-quadruplex fully formed. After that, the electrode was thoroughly washed with 0.10 M PBS to remove unbound Pb²⁺. The obtained electrode was denoted as Pb²⁺-ssDNA/CH-NbNiO-MWCNTs/ITO.

2.7 Electrochemical measurements

Electrochemical measurements were investigated by cyclic voltammetry (CV), electrochemical impedance spectroscopy (EIS) and differential pulse voltammetry (DPV). The CV scans were performed at 10mV/s from -0.4 to 0.8V (vs. Ag/AgCl). EIS measurements were conducted at 0.18V over a 10⁻²-10⁵ Hz frequency range, with 0.01V signal amplitude. DPV currents were obtained over a potential range from -0.15 to 0.55V with pulse amplitude of 0.025V. Electrochemical measurements were carried out in a 0.1 M phosphate buffer solution (PBS, pH 7.0) containing 5 mM [Fe(CN)₆]^{3-/4-} solution and 0.1 M KCl solution. The detailed fabrication and detection procedures for the developed DNA biosensor are illustrated in Fig. 1.

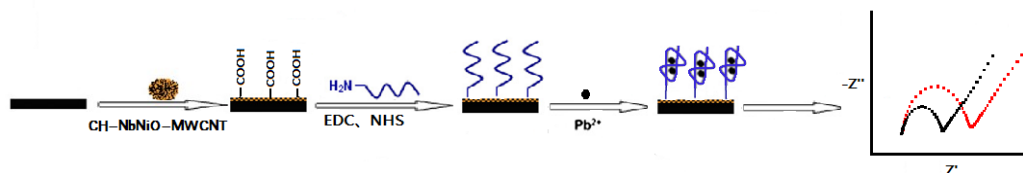


Figure 1. Schematic representation of the steps for fabrication of DNA biosensor

3. RESULTS AND DISCUSSION

3.1 Optimization of the synthesis conditions

3.1.1 The choice of dopant

In order to compare the conductivity of NiO nanomaterials doped with different metal elements, the electrochemical properties of the different modified electrodes were characterized by cyclic voltammetry. The experimental results showed that the peak current of Nb-doped NiO was much higher than that of NiO doped with other elements. Thus, the NbNiO was chosen for further studies.

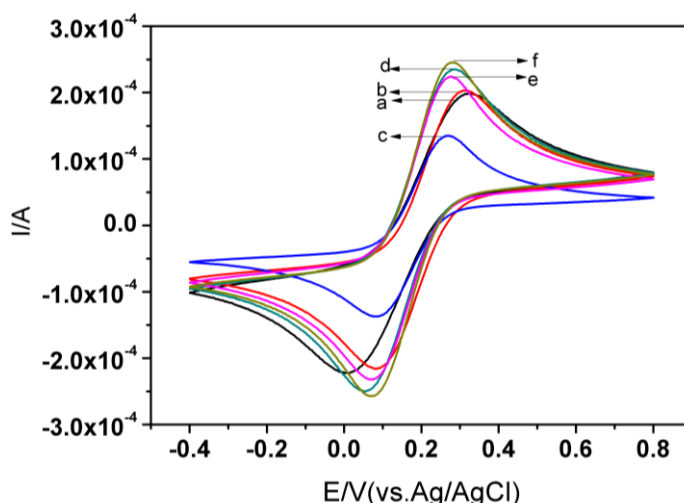


Figure 2. The CVs of different metal doped NiO modified ITO electrode. (a)CH/ITO, (b)NiO/ITO, (c)MnNiO/ITO, (d)TiNiO/ITO, (e)VNiO/ITO and (f)NbNiO/ITO in 0.1 M phosphate buffer solution (PBS, pH 7.0) containing 5 mM $[\text{Fe}(\text{CN})_6]^{3-/4-}$ solution and 0.1 M KCl solution with scan rate of 10mV/s.

3.1.2 The optimization of dopant content

In order to investigate the effect of dopant (Nb) content on the conductivity of NbNiO nanoparticles, we synthesized different proportion of Nb-doped NiO nanoparticles by sol-gel method

and investigated by cyclic voltammetry. As seen in Fig.3, the peak current of pristine NiO was much lower than that of NiO doped with Nb, which suggested that doping Nb could improve the conductivity of the electrode. When the content of Nb was ten percent (wt.%), the maximum peak current was achieved. Thus, the optimal doping ratio was 10%.

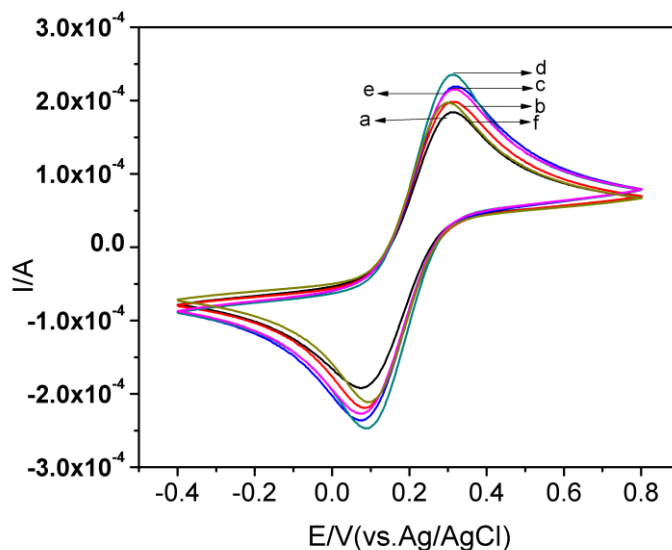


Figure 3. The CVs of NbNiO modified ITO electrode with various Nb contents. (a)un-doped, (b)5%, (c)8%, (d)10%, (e)12%, (f)15% in 0.1 M phosphate buffer solution (PBS, pH 7.0) containing 5 mM $[\text{Fe}(\text{CN})_6]^{3-/4-}$ solution and 0.1 M KCl solution with scan rate of 10mV/s.

3.2 Characterization of NbNiO

3.2.1 XRD characterization

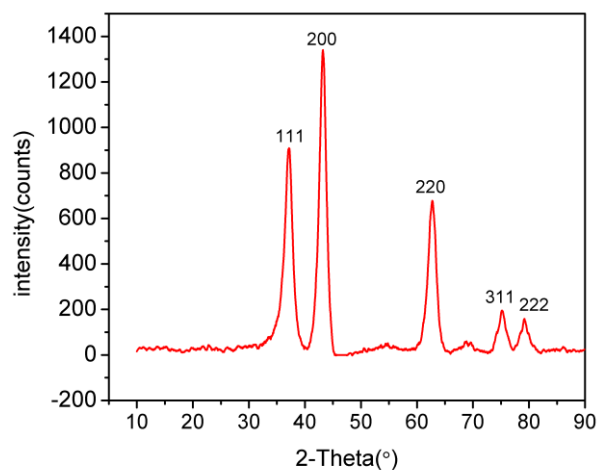


Figure 4. X-ray powder diffraction pattern of NbNiO.

The phases of the synthetic NbNiO samples were investigated by XRD analysis. As can be seen from Fig. 4, the diffraction peaks corresponding to (111), (200), (220), (311) and (222) planes were observed. All of these diffraction peaks of NiO can be indexed as a face-centered cubic phase as identified using the standard date JCPDS04-0835. No any other impurities were observed in the powder pattern, indicating that the Nb was doped into crystallographic structure of NiO.

3.2.2 SEM characterization

To further illustrate our synthesis strategy, the product was also characterized by SEM. The SEM image of the sample was shown in Fig.5. It can be seen that the samples showed irregular shapes with an average size of about 30~50 nm. A three-dimensional structure was formed among particles indicating a large specific surface area. The BET surface area was also determined by N₂ physisorption exhibiting a reasonably high specific surface area of 160.41 m² g⁻¹, which was consistent well with SEM results.

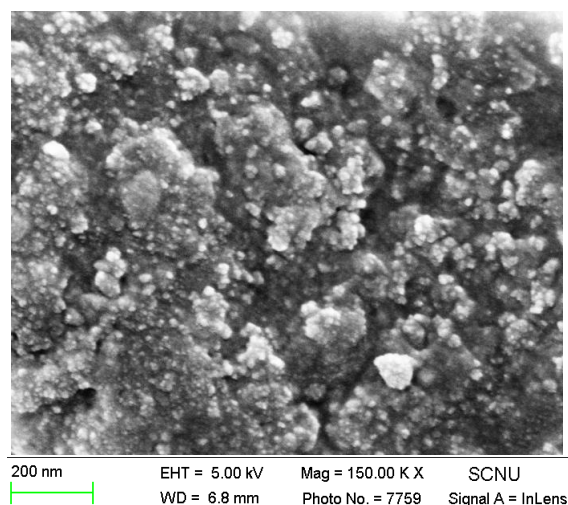


Figure 5. SEM image of NbNiO nanoparticles

3.3 Characterization of the modified electrodes

3.3.1 SEM characterization

The morphologies and microstructures of different modified electrodes were studied by means of SEM as shown in Fig. 6. From Fig. 6A, the obtained MWCNTs was stacked together and constituted a reticulated porous nanostructure, measuring about 50 nm in mean diameter. After adding chitosan, we could see that the surface of MWCNTs was uniformly coated with a layer of chitosan membrane (Fig. 6B). Fig. 6C displayed the surface of CH-NbNiO-MWCNTs nanocomposites. As can be seen from it, NbNiO nanoparticles were uniformly dispersed in the network structure of carbon nanotubes, which is conducive to improve the conductivity of the electrode and capture more DNA

molecules. When the CH-NbNiO-MWCNTs nano-composites were conjugated with ssDNA, as Fig 6D shown, the nanocomposites matrix were buried under layer of immobilized DNA and was attributed to very high loading of the probe DNA molecules on the surface of the modified electrode.

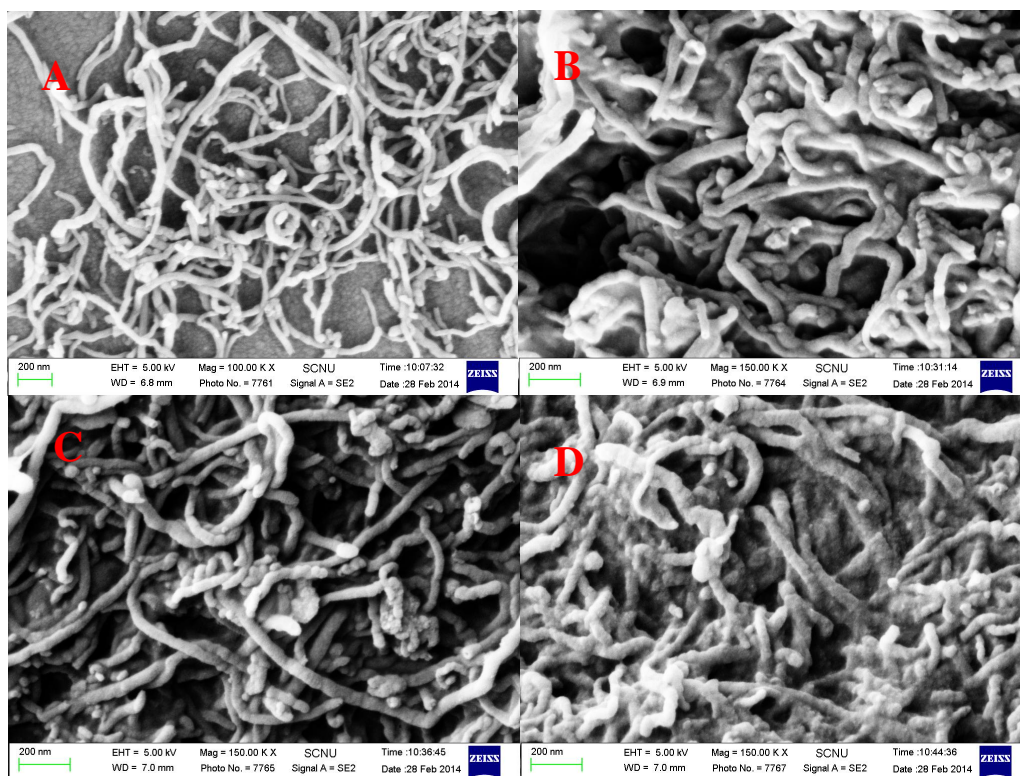


Figure 6. SEM images of (A) MWCNTs, (B) MWCNTs-CH, (C) CH-NbNiO-MWCNTs and (D) ssDNA/CH-NbNiO-MWCNTs on the surface of ITO.

3.3.2 Electrochemical characterization

Electrochemical impedance spectroscopy (EIS) is an effective method to monitor the interface properties of the electrodes in the assembly process and was widely used to characterize the fabrication process of DNA biosensor[33]. Fig. 7A shows the impedance spectroscopy of stepwise assembly procedures. Results revealed that NbNiO-CH (curve c) and MWCNTs-CH (curve d) modified electrodes showed a lower electron transfer resistance (R_{et}) than the CH modified one (curve b), implying that NbNiO and MWCNTs possessed excellent electron transfer property and were able to accelerate the electron transfer. When the NbNiO and MWCNTs were added simultaneously, R_{et} of the CH-NbNiO-MWCNTs/ITO electrode (curve e) achieved minimum, indicating the synergistic effect of NbNiO and MWCNTs. After ssDNA was conjugated (curve f), R_{et} increased due to the electrostatic repulsion between the negatively charged phosphate backbones of probe ssDNA and $[\text{Fe}(\text{CN})_6]^{3-/4-}$ anion[34], confirming the effective immobilization of ssDNA. In the presence of Pb^{2+} , R_{et} increased sharply (curve g). It was probably due to Pb^{2+} induced the G-rich DNA conformational switch from a random-coil to G-quadruplex. Meanwhile, differential pulse voltammetry also applied to characterize various modified electrodes, which coincided with the EIS results.

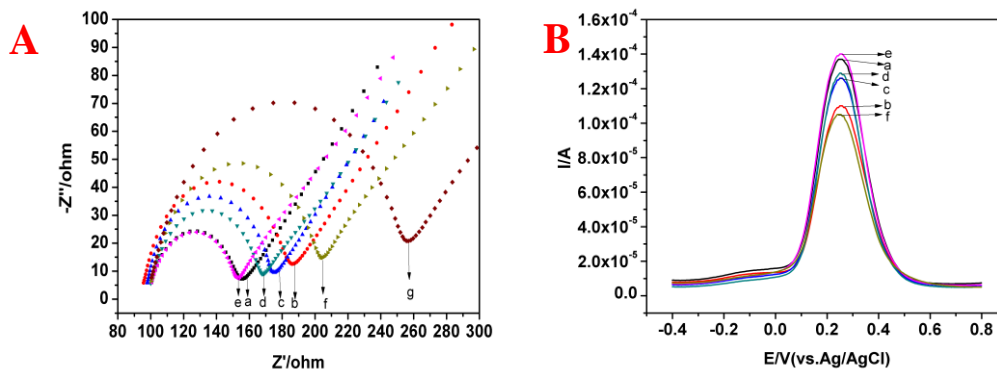


Figure 7. EIS and DPV of (a)ITO electrode,(b)CH/ITO electrode, (c)NbNiO-CH/ITO lectrode, (d)MWCNTs-CH/ITO electrode, (e)CH-NbNiO-MWCNTs/ITOelectrode,(f)ssDNA/CH-NbNiO-MWCNTs/ITOand(g)Pb²⁺-ssDNA/CH-NbNiO-MWCNTs/ITO.

3.4 Optimization of pH

The effect of pH value on the formation of G-quadruplex was studied, due to the great influence of pH on the biological activity and stability of biological molecules. The relation curve of pH values and the R_{et} difference (ΔR_{et}) before and after the formation of G-quadruplex was shown in Fig. 8. It was found that the change of supporting solution's pH would cause obviously change of ΔR_{et} . The value of ΔR_{et} increased with the increasing pH value from 6.0 to 7.0 and then decreased when the pH exceeded 7.0. Thus, pH 7.0 of the working buffer was selected for the further studies.

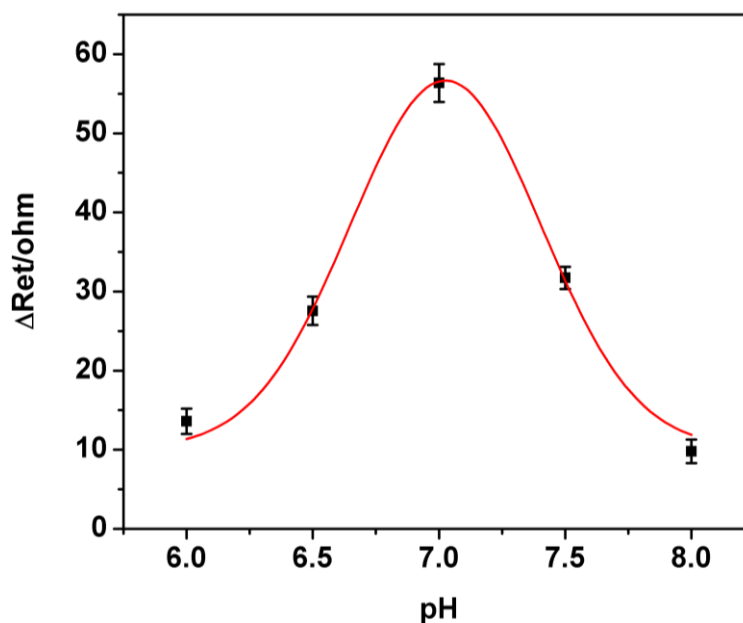


Figure 8. The effect of pH on the performance of the biosensor was examined from 6.0 to 8.0.

3.5 Sensitivity and Selectivity

Under optimal conditions, the sensitivity of the DNA biosensor was studied by immersing into various concentrations of Pb²⁺ solution.

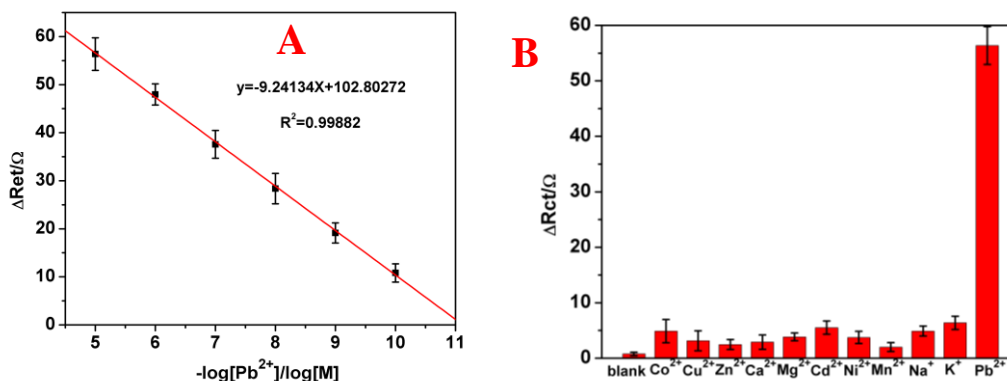


Figure 9. The calibration plot of ΔR_{et} vs negative logarithm of Pb²⁺ concentrations and selectivity (B) with 10 μ M metal ion (such as 10 μ M Co²⁺, Cu²⁺, Zn²⁺, Ca²⁺, Mg²⁺, Cd²⁺, Ni²⁺, Mn²⁺, Na⁺, K⁺).

Table 1. Comparison performance of this proposed biosensor with that of some other DNA biosensors for Pb²⁺ detection

| Probe | Detection method | Linear range (M) | LOD(M) | References |
|---|------------------|---|------------------------|-----------------|
| G-quadruplex/Amplex ultrared | Fluorescence | 0~10 ⁻⁶ | 4×10 ⁻¹⁰ | Li et al. 2011 |
| G-quadruplex/AuNPs | Fluorescence | 0~10 ⁻⁶ | 1.28×10 ⁻¹⁰ | Ho et al. 2013 |
| TBA/CeO ₂ -MWCNTs-EMIMBF ₄ /GCE | Amperometry | 10 ⁻⁸ ~10 ⁻⁵ | 5.0×10 ⁻⁹ | Li et al. 2011 |
| G-quadruplex | EIS | 5×10 ⁻¹⁰ ~5×10 ⁻⁵ | 5.0×10 ⁻¹⁰ | Lin et al. 2011 |
| Pb ²⁺ -ssDNA/CH-NbNiO-MWCNTs/ITO | EIS | 10 ⁻¹⁰ ~10 ⁻⁵ | 7.51×10 ⁻¹² | proposed |

When Pb²⁺ interaction with G-rich DNA to form G-quadruplex, it would hinder electron transfer, resulting in an increase of R_{et}. As shown in Figure 9A, upon decreasing the concentration of Pb²⁺ from 10⁻⁵ M to 10⁻¹⁰ M, the ΔR_{et} gradually decreased, because less and less ssDNA on the electrode could form G-quadruplex. ΔR_{et} decreased linearly with the logarithm of Pb²⁺ concentration within a range from 10⁻⁵ M to 10⁻¹⁰ M. The linear regression equation was as follows:

$$\Delta R_{et}(\Omega) = 9.24 \log C_{Pb^{2+}}(\text{mol} \cdot \text{L}^{-1}) + 102.80 \quad R^2 = 0.998$$

Where, ΔR_{et} was the R_{et} difference before and after the ssDNA interactions with Pb²⁺; C_{Pb2+} was the concentration of Pb²⁺; R was the correlation coefficient.

The detection limit of the assay for Pb^{2+} detection was determined to be 7.51×10^{-12} M (3σ) (where σ is the relative standard deviation of the blank solution, $n=11$), which is lower than those of electrochemical, fluorescent, and colorimetric assays for Pb^{2+} .

The selectivity of the biosensor was also explored: the values of ΔR_{et} were analyzed upon adding other metal ions (such as $10 \mu\text{M}$ Co^{2+} , Cu^{2+} , Zn^{2+} , Ca^{2+} , Mg^{2+} , Cd^{2+} , Ni^{2+} , Mn^{2+} , Na^+ , K^+) to the sensing system instead of Pb^{2+} . The result was shown in Fig. 9B. We observed that only Pb^{2+} caused a considerable decrease in R_{et} while other ions yielded little changes, which indicated that the sensor was specifically responding to the Pb^{2+} . The good performance of the DNA biosensor in comparison with other DNA biosensor is obvious from Table 1. It is clear that the different characteristics of the proposed strategy for Pb^{2+} detection are better in some cases or comparable with the other sensors reported so far.

3.6 Application of the biosensor

To evaluate the analytical reliability and application potential of the developed biosensor, recovery experiments for pure drinking water with different Pb^{2+} concentrations were performed. The results summarized in Table 2 showed that the biosensor showed an acceptable accuracy, with RSD values ranging between 0.2 and 2.4. Simultaneously, the Pb^{2+} recovery was between 99.0% and 102.4%, which clearly indicated the potentiality of the biosensor for detection of Pb^{2+} in environmental monitoring with the proposed method.

Table 2. Recoveries of Pb^{2+} in drinking water samples spiked with Pb^{2+} standard solution

| Sample | Concentration (M) | | RSD (% , n=5) | Recovery (%) |
|--------|------------------------|----------------------------------|---------------|--------------|
| | Added | Found | | |
| 1 | 0 | Not Found | -- | -- |
| 2 | 5.00×10^{-6} | $4.95(\pm 0.05) \times 10^{-6}$ | 1.0 | 99.0 |
| 3 | 5.00×10^{-7} | $5.05(\pm 0.10) \times 10^{-7}$ | 2.0 | 101.0 |
| 4 | 5.00×10^{-8} | $5.12(\pm 0.08) \times 10^{-8}$ | 1.6 | 102.4 |
| 5 | 5.00×10^{-9} | $5.03(\pm 0.01) \times 10^{-9}$ | 0.2 | 100.6 |
| 6 | 5.00×10^{-10} | $4.98(\pm 0.12) \times 10^{-10}$ | 2.4 | 99.6 |

4. CONCLUSIONS

In summary, a novel electrochemical biosensor for highly sensitive detection of Pb^{2+} has been developed utilizing CH-NbNiO-MWCNTs nanocomposite as a promising transduction platform. The NbNiO nanoparticles possessed a large specific surface area could greatly enhance the immobilization of DNA probes and synergistic improve the electrical conductivity with the MWCNTs. The detection of Pb^{2+} was based on Pb^{2+} induced the conformation of G-rich DNA to switch from a random-coil to G-quadruplex and result in an increase of alternating current impedance. Result showed that the

biosensor has high sensitivity, low detection limit, good selectivity and a wide linear range for the quantitative analysis of Pb^{2+} . The assay can be used in environmental monitoring and analysis.

ACKNOWLEDGEMENTS

The authors wish to thank the Science and Technology Planning Project of Guangzhou (No.2009Z2-D511), China, for their financial support.

References

1. E. Herrero, V. Arancibia, C. Rojas-Romo, *J. Electroanal. Chem.*, 729 (2014) 9.
2. F. Zapata, A. Caballero, A. Espinosa, A. Tarraga, P. Molina, *Organic Letters*, 10(2008)41.
3. M.B. Dessuy, R.M. de Jesus, G.C. Brandao, S.L.C.Ferreira, M.G.R. Vale, B. Welz, *Food Additives and Contaminants Part a-Chemistry Analysis Control Exposure & Risk Assessment*, 30 (2013) 202.
4. S. Gunduz, S. Akman, *Regulatory Toxicology and Pharmacology*, 65(2013)34.
5. M. Shamsipur, N. Fattahi, M. Sadeghi, M. Pirsaeheb, *J. Iranian Chemical Society*, 11(2014) 249.
6. F. Queroue, A. Townsend, P. van der Merwe, D. Lannuzel, G. Sarthou, E. Bucciarelli, A. Bowie, *Analytical Methods*, 6(2014)2837.
7. S. Yenisoy-Karakas, *Food Chemistry*, 132(2012)1555.
8. N. Zhang, H. Peng, S. Wang, B. Hu, *Microchimica Acta*, 175(2011)121.
9. L. Zhu, L. Xu, B. Huang, N. Jia, L. Tan, S. Yao, *Electrochimica Acta*, 115(2014)471.
10. Z.Y. Kong, J.F. Wei, Q.J. Fan, Y.H. Li, K.Y. Zhao, H.T. Guo, C.M. Wei, *Analytical Methods*, 5 (2013) 4905.
11. S.J. Li, N. Xia, X.L. Lv, M.M. Zhao, B.Q. Yuan, H. Peng, *Sensors and Actuators B (Chem.)*, 190(2014)809
12. Z. Zhu, J. Liu, S. Zhang, X. Na, X. Zhang, *Spectrochimica Acta Part B-Atomic Spectroscopy* 63(2008) 431
13. C.L. Li, K.T. Liu, Y.W. Lin, H.T. Chang, *Analytical Chemistry* 83(2011)225
14. G. Munteanu, S. Munteanu, D.O. Wipf, *J. Electroanalytical Chemistry*, 632(2009)177
15. A.K. Brown, J. Li, C.M.B. Pavot, Y. Lu, *Biochemistry*, 42 (2003)7152
16. L. Zhang, B. Han, T. Li, E. Wang, *Chemical Communications*, 47 (2011)3099
17. A.T. Phan, V. Kuryavyi, D.J. Patel, *Current Opinion in Structural Biology*, 16(2006) 288
18. Z. Lin, Y. Chen, X. Li, W. Fang, *Analyst*, 136(2011)2367
19. S.Iijima, *Nature*, 354(1991)56
20. J. Lin, W. Qu, S. Zhang, *Analytical Biochemistry*, 360 (2007) 288
21. T.A.N. Peiris, H. Alessa, J.S. Sagu, I.A. Bhatti, P. Isherwood, K.G.U. Wijayantha, *J. Nanoparticle Research*, 15(2013)2115
22. S.J. Choi, B.H. Jang, S.J. Lee, B.K. Min, A. Rothschild, I.D. Kim, *ACS Applied Materials & Interfaces*, 6(2014) 2588
23. W.J. Tseng, T.T. Tseng, H.M. Wu, Y.C. Her, T.J. Yang, *J. American Ceramic Society*, 96(2013)719
24. Z. Li, L. Chen, F. He, L. Bu, X. Qin, Q. Xie, S. Yao, X. Tu, X. Luo, S. Luo, *Talanta*, 122(2014) 285
25. J. Feng, S. Xiong, Y. Qian, L. Yin, *Electrochimica Acta* 129(2014)107
26. B. Zhao, X.K. Ke, J.H. Bao, C.L. Wang, L. Dong, Y.W. Chen, H.L. Chen. *J. Physical Chemistry C*, 113(2009)14440
27. Y. Wu, Y.M. He, T.H. Wu, T. Chen, W.Z. Weng, H.L. Wan, *Materials Letters*, 61(2007)3174
28. Y. Wu, Y.M. He, T.H. Wu, W.Z. Weng, H.L. Wan, *Materials Letters*, 61(2007)2679

29. J.B. Wu, C.W. Nan, Y.H. Lin, Y.Deng, *Physical Review Letters*, 89(2002) 217601
30. J. Wu, C.W. Nan, Y.H. Lin, Y. Deng, *Physical Review Letters*, 89(2002)217601
31. W. Zhang, T. Yang, X. Zhuang, Z. Guo, K. Jiao, *Biosensors & Bioelectronics*, 24(2009)2417
32. F.F. Deng, C. Ding, Y. Wang, W.T. Li, L.L.Liu, H. Li, *Anal. Methods*, 6(2014) 9228
33. Z.Y. Guo, T.T. Hao, S.P. Du, B.B. Chen, Z.B. Wang, X. Li, S. Wang, *Biosensors & Bioelectronics*,44(2013)101
34. M. Tak, V. Gupta, M. Tomar, *Biosensors & Bioelectronics*,59(2014)200

© 2015 The Authors. Published by ESG (www.electrochemsci.org). This article is an open access article distributed under the terms and conditions of the Creative Commons Attribution license (<http://creativecommons.org/licenses/by/4.0/>).